

The Influence of Diodes and Transistors Made of Silicon and Silicon Carbide on the Nonisothermal Characteristics of Boost Converters

Krzysztof Górecki, Janusz Zarębski

Gdynia Maritime University, Department of Marine Electronics, Poland

Abstract: In the paper the results of simulations and measurements of the boost converter operating with silicon and silicon carbide devices are presented. SPICE simulations were performed with the use of electrothermal hybrid models of unipolar transistors and Schottky diodes. The influence of the input voltage, the pulse-duty factor and the load resistance of the boost converter including silicon MOSFET, silicon Schottky diode, silicon carbide Schottky diode and silicon carbide MESFET on characteristics of this converter are analysed. The simulation results are verified experimentally. On the basis of obtained results of calculations and measurements, the influence of selection of the considered semiconductor devices on the boost converter characteristics is discussed.

Key words: Boost converter, SiC semiconductor devices, steady state characteristics, modelling

Vpliv diod in tranzistorjev iz silicija in silicijevega karbida na neizotermične karakteristike stikalnega pretvornika navzgor

Povzetek: V članku so predstavljeni rezultati in meritve stikalnega pretvornika navzgor z elementi iz silicija in silicijevega karbida. Izvedene so bile SPICE simulacije z uporabo elektrotermičnih hibridnih modelov unipolarnega tranzistorja in schottkyjevih diod. Analiziran je vpliv vhodne napetosti, razmerja med pulzom in premorom in upornosti bremena stikalnega pretvornika navzgor s silicijevim MOSFET, silicijevo schottky diodo, schottky diodo iz silicijevega karbida in MESFET iz silicijevega karbida na karakteristike pretvornika. Simulacije so eksperimentalno preverjene. Na osnovi izračunov in meritev je obrazložen vpliv izbranih elementov na lastnosti stikalnega pretvornika.

Ključne besede: stikalni pretvornik, polprevodniški elementi iz SiC, statična karakteristika, modeliranje

* Corresponding Author's e-mail: gorecki@am.gdynia.pl

1. Introduction

The non-isolated boost converter – NBC (Fig.1) belongs to a class of power electronic circuits most often used. The NBC is applied both in supplying circuits and power factor correction (PFC) circuits [1 - 7]. Properties of the considered converter depend on parameter values of the component elements, especially – semiconductor power devices, e.g. [6 - 12].

Typically, silicon power devices are used in boost converters, but recently more and more papers describe

such circuits with silicon carbide (SiC) devices [2 – 4, 10 - 17]. The properties of silicon carbide power semiconductor devices are presented in many papers, e.g. in [7, 18 – 25]. In the cited papers, it is underlined that SiC power semiconductor devices can operate in higher temperature and with higher switching frequency than classical silicon semiconductor devices. In the papers [2 – 4, 10 – 15, 17] the switching converters including SiC Schottky diodes, power JFETs, power BJTs or power MOSFETs are described. The considered converters are utilized in PFC circuits, photovoltaic (PV) systems, inverters for IPM traction drive or other high frequency

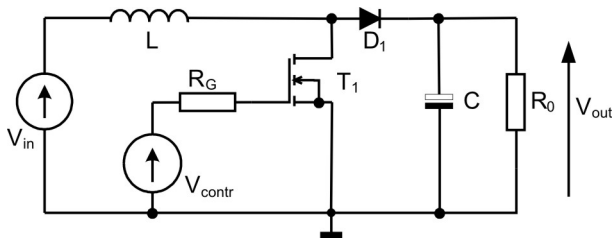


Figure 1: The non-isolated boost converter

and high voltage power networks. The authors of the cited papers proved that using SiC semiconductor power devices make possible to reduce power losses in high voltage switching converters [26].

Nowadays, specialist computer programs along with devices models are used in the process of analysing and designing electronic circuits. SPICE is one of the most popular tools used for this purpose [1, 27-30].

One of the essential physical phenomena influencing the devices and dc-dc converters characteristics is selfheating [1, 8, 27, 30 - 35]. To take into account such a phenomenon in the circuits' analysis, the device electrothermal models have to be used. Due to some properties of pulse circuits, the electrothermal models have to model, first of all, the device ON and OFF states. Apart from this, such models should have possibly relative short time of calculations. Unfortunately, the so called global electrothermal models (GETM) [24, 36 - 41] do not possess such properties and therefore GETMs are not suitable to analyse dc-dc converters. The GETMs are the complex model, which describe properties of semiconductor devices very accurately using the network form composed of passive components and controlled current or voltage sources. For example, some attempts to use the GETM of Schottky diode [36] and MESFET [37] lead to unconvergency of calculations.

In turn, as it was shown in [8, 30, 42, 43, 47], the hybrid electrothermal models (HETM) assure both high accuracy and acceptable time of calculations. Such models consist of two parts. First of them is the isothermal model built-in in SPICE whereas the second part includes controlled current or voltage sources modelling the influence of the increase of the internal device temperature on its terminal currents and voltages. Forms of such models for the considered devices are presented in the next section.

In this paper, which is the extended version of the paper [44], properties of boost converters with unipolar transistors and Schottky diodes made of silicon and silicon carbide are compared. The theoretical considerations are illustrated by some results of the calculations and measurements.

2. Electrothermal hybrid models of unipolar transistors and diodes

The hybrid electrothermal models of semiconductor devices dedicated for SPICE were presented for example in [8, 30, 43, 44]. HETM consists of the isothermal device model built-in in SPICE, the controlled voltage sources modelling the additional voltage drops between the device terminals resulting from selfheating and the compact device thermal model making it possible to calculate the device internal temperature, based on the device dissipated power course and the course of the device transient thermal impedance.

Fig. 2 illustrates the network representation of the hybrid linear model of the diode, in which the influence of the temperature on the voltage drop across the forward biased junction and the series resistance is taken into account.

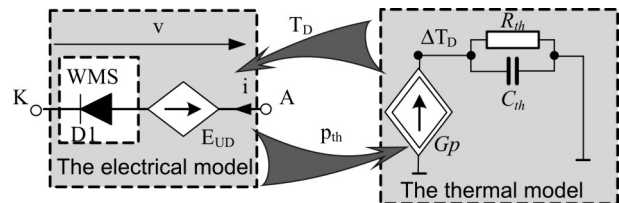


Figure 2: The circuit representation of the hybrid electrothermal model of the diode

In this model D1 represents the isothermal diode model built-in in the SPICE program [45], the controlled voltage source E_{UD} models the temperature changes of the voltage across the forward biased junction and on the diode series resistance.

The value of the source E_{UD} is given by the formula

$$E_{UD} = i \cdot RS \cdot \alpha_{RS} \cdot (T_D - T_0) + \alpha_U \cdot (T_D - T_0) \quad (1)$$

where RS designates the series resistance of the diode at the reference temperature T_0 , α_{RS} is the temperature coefficient of relative changes of this resistance, α_U is the temperature coefficient of the voltage changes on the forward biased junction, whereas T_D denotes the internal temperature of the diode.

The compact thermal model is composed of the source Gp , the current of which is equal to the device thermal power p_{th} and the two-terminal R_{th} , C_{th} modelling the device transient thermal impedance. To reduce the time of calculations only one thermal time constant of the non-physical value characterizing the device transient thermal impedance was used in the model [8, 30]. The power model is given by the formula

$$p_{th} = v \cdot i \quad (2)$$

In turn, the circuit representation of the electrothermal hybrid linear model of the unipolar transistor, in which the dependence of the series resistance of the drain on the temperature is taken into account, is shown in Fig.3.

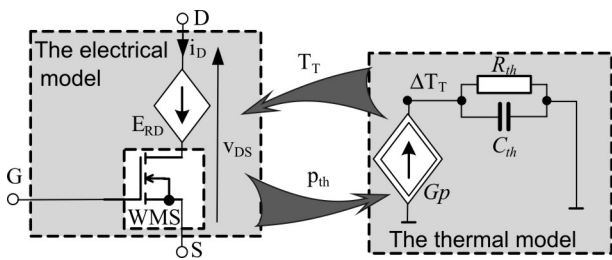


Figure 3: The circuit representation of the hybrid electrothermal model of the MOSFET transistor

In Fig.3 WMS stands for the isothermal model of the MOSFET transistor built-in in the SPICE software [45], the controlled voltage source E_{RD} models the dependence of the series resistance of the drain on temperature.

The value of the source E_{RD} is given by the formula

$$E_{RD} = i_D \cdot R_{ON} \cdot \alpha_{RD} \cdot (T_T - T_0) \quad (3)$$

where R_{ON} designates the value of the transistor on-state resistance at the reference temperature T_0 , α_{RD} is the temperature coefficient of the relative changes of this resistance, whereas T_T denotes the internal temperature of the transistor.

The power model is given by the formula

$$p_{th} = v_{DS} \cdot i_D \quad (4)$$

where the voltage v_{DS} and the current i_D are marked in Fig.3.

In both the presented models the internal device temperature (T_T for the transistor and T_D for the diode) is the sum of the ambient temperature T_a and the temperature excess (ΔT_T for the transistor and ΔT_D for the diode) calculated from the thermal model.

3. Results

In this Chapter the results of experimental verification of the electrothermal hybrid models of the diode and the unipolar transistor (see Chapter 2) as well as the boost converter with these devices are presented. The investigations were performed for four devices: the silicon Schottky diode 1N5822, the silicon carbide Schott-

ky diode SDP04S60, the silicon MOSFET IRF540 and the silicon carbide MESFET CRF24010.

The parameter values of the electrothermal hybrid models of the considered devices are collected in Appendix.

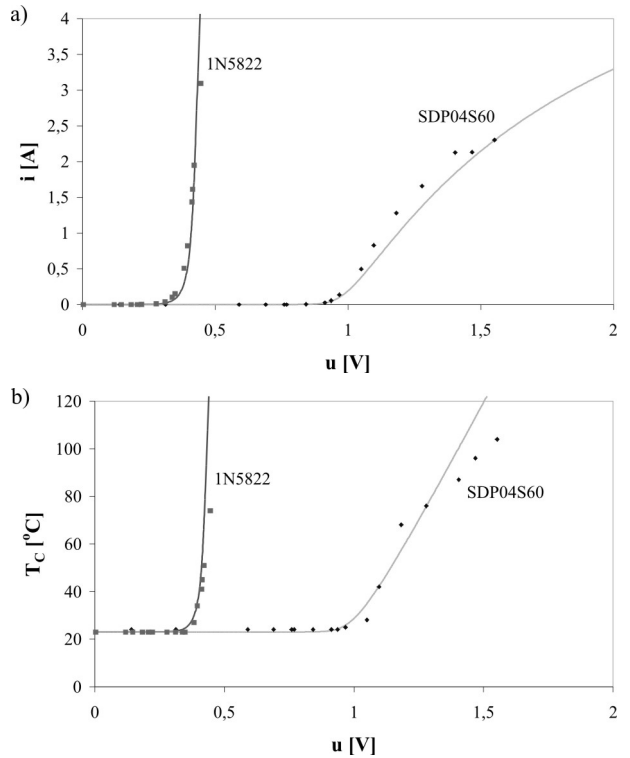


Figure 4: The nonisothermal dc characteristics of the considered Schottky diodes (a) and the dependence of the case temperature of these diodes on their voltage-drop (b)

In Figs.4-5 the nonisothermal dc characteristics of the forward biased diodes (Fig.4) and the transistors in the non-saturation region (Fig.5) are presented. In these figures points denote results of measurements, whereas lines denote results of calculations. As seen, a good agreement between the calculated and measured characteristics was obtained, which confirms high correctness of both the proposed models and the procedure of model parameters values estimation. It is worth mentioning that the voltage drops on the SiC devices switched-on are much greater than on their silicon counterparts. For example, the voltage drop on the forward biased silicon carbide diode is twice higher than on the silicon one. Apart from this, the SiC diode possesses several times higher value of the series resistance than their silicon counterpart. Consequently, the voltage drop on the SiC diode at the forward current equal to 2.5 A is over four times higher than that on the silicon diode.

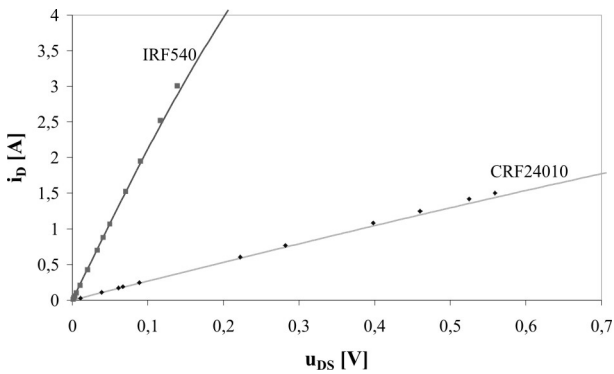


Figure 5: The nonisothermal dc output characteristics of the considered unipolar transistors operating in the non-saturation range

In turn, as it is seen in Fig.5, the slope of the output characteristic $i_D(v_{DS})$ equal to the transistor channel resistance is hardly ten times smaller for the silicon transistor than for the SiC MESFET. This difference of the voltage-drop causes directly much higher energy losses in the switched-on SiC MESFET than in the comparable silicon transistor.

Using the investigated devices, the influence of their properties on the boost converter characteristics was examined.

The investigated boost converter contains: the coil $L = 330 \mu\text{H}$, the capacitor $C = 220 \mu\text{F}$ and three sets of semiconductor switching devices. The first set, called here the converter CONV1, consists of the silicon power MOSFET (IRF540) and the silicon Schottky diode (1N5822). The second set (CONV2) consists of the silicon MOSFET (IRF540) and the SiC-Schottky diode (SDP04S60). The third set (CONV3) consists of the power transistor SiC-MESFET (CRF24010) and the SiC-Schottky diode (SDP04S60). The control signal, represented in Fig.1 by the voltage source V_{contr} is generated by the monolithic PWM controller (UC3842). The MOSFET transistor is controlled directly by this controller, whereas to control the MESFET transistor the circuit shifting the control voltage [13] is additionally used. During investigations, both the transistors were situated on the heat-sink of dimensions $50 \times 100 \times 10 \text{ mm}$, whereas both the diodes operated without any heat-sink.

Using the electrothermal SPICE models of the considered devices shown in Figs. 2, 3 the characteristics of the boost converter at the steady state were simulated with the use of the analysis method described in [46]. Moreover, such characteristics were measured. The following dependences were considered: the dependence of the output voltage and the watt-hour efficiency of the converter and the case temperature of the semiconductor devices (transistors and diodes) on the input

voltage, the load resistance and the pulse duty factor of the control signal. The investigations were performed at the typical control signal frequency equal to 100 kHz. The output voltage was measured directly using digital voltmeter, the watt-hour efficiency was obtained indirectly based on the measured RMS values of the converter input and output currents and voltages, whereas the case temperatures of the transistor and the diode were measured using the thermo-hunter.

In Figs.6-8 some results of the investigations are presented. In these figures, the results of calculations and measurements are marked by lines and points, respectively. As seen, the obtained characteristics have a very similar shape for all the considered converters - only the quantitative differences between the characteristics are observed.

It is worth mentioning that on the dependence $V_{\text{out}}(d)$ the maximum is observed, whereas the dependence $\eta(d)$ is a monotonically decreasing function. As it was proved in [35] the value of this maximum depends on the on-resistance R_{ON} of the power transistor channel. In the considered case, R_{ON} for the MOSFET is 10 times lower than for the MESFET and the maximum value of the output voltage V_{out} of the converter CONV1 is of about 25% higher than the output voltage of the converter CONV3. This difference causes also the lower value of the watt-hour efficiency of the converter CONV3. On the other hand, the forward voltage-drop of the silicon Schottky diode is much lower than the forward voltage-drop of the silicon carbide Schottky diode. This difference causes, that the case temperature of SiC Schottky diodes operating in the converters CONV2 and CONV3 is much higher than the case temperature of silicon Schottky diode operating in the converter CONV1.

In turn, it results from the dependence $V_{\text{out}}(R_o)$ that the converters CONV1 and CONV2 operate in the continuous conducting mode in all the considered range of changing of the load resistance R_o , whereas the converter CONV3 starts operating in the discontinuing current mode for $R_o > 800 \Omega$. For all the considered converters the increasing functions $V_{\text{out}}(R_o)$ and $\eta(R_o)$ is observed. On the other hand, the case temperatures of the diodes and transistors are the monotonically decreasing functions of the load resistance. The load resistance cannot be lower than 10Ω , because at this value of the resistance R_o , the diode case temperature is nearly the catalogue admissible value. Note, that much higher energy losses existing in the transistors as compared with diodes do not cause the essentially higher values of the transistor internal and case temperatures due to the fact that the value of the diode thermal resistance is of much higher value than the value of the

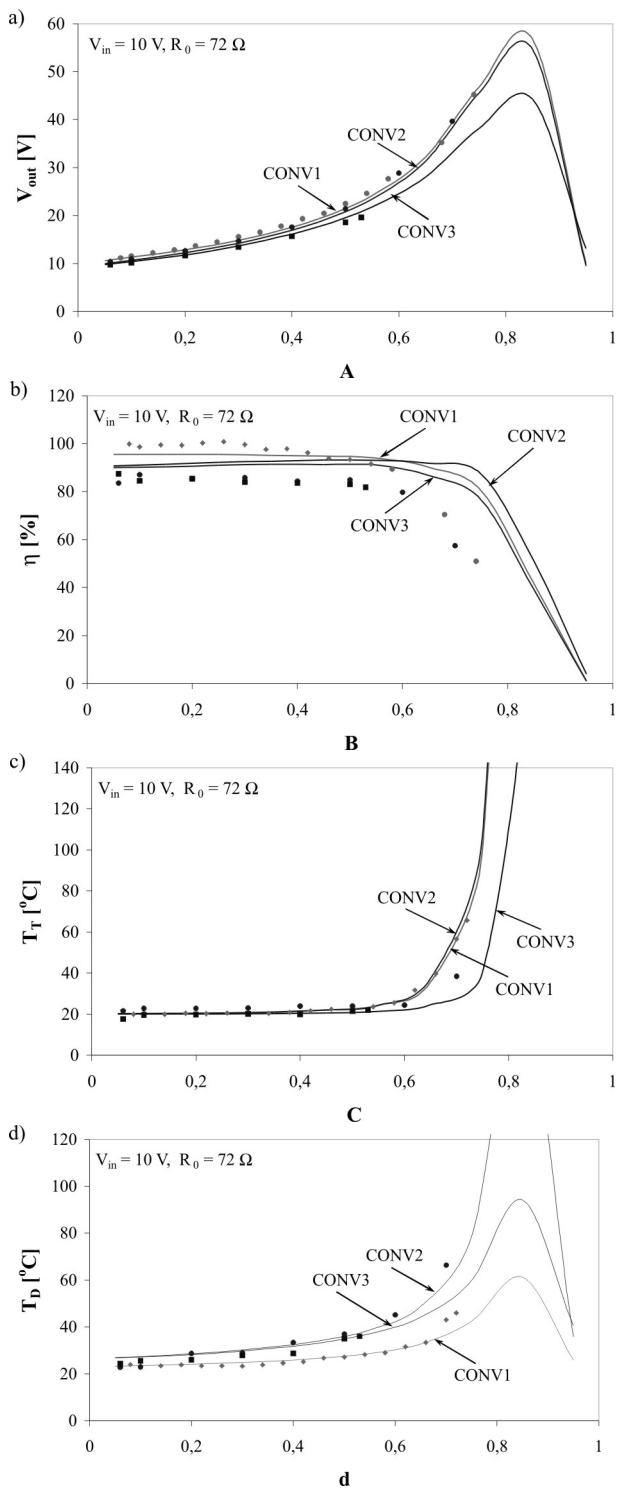


Figure 6: Dependences of the converter output voltage (a), the watt-hour efficiency (b), the transistor case temperature (c) and the diode case temperature (d) on the pulse duty factor d of the control signal

transistor thermal resistance. As it is seen, for all the investigated converters a good agreement between the results of measurements and analyses was obtained for the load resistance $R_0 > 10\ \Omega$, which confirms the correctness of the device models used in the analyses.

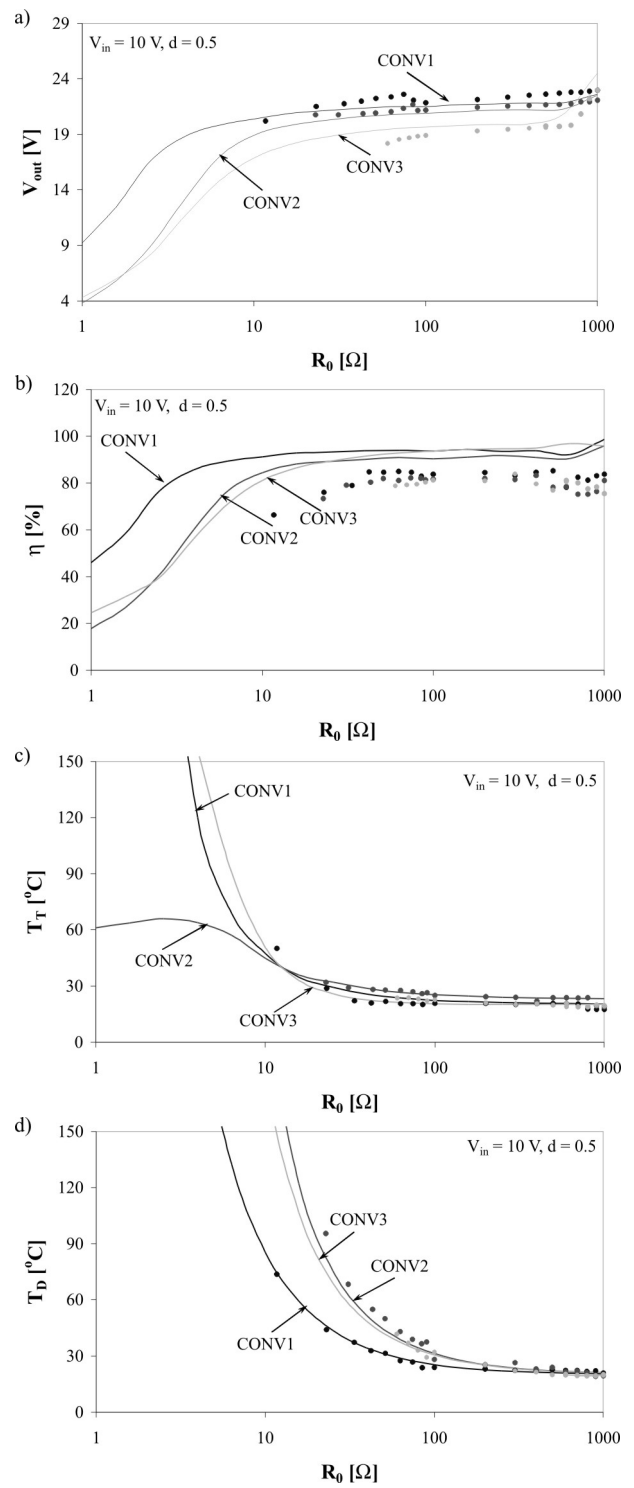


Figure 7: Dependences of the converter output voltage (a), the watt-hour efficiency (b), the transistor case temperature (c) and the diode case temperature (d) on the load resistance

Additionally, the influence of the input voltage of the considered parameters of the boost converter was investigated. The range of change of the converter input voltage was limited by the admissible drain-source voltage of the SiC MESFET. In the range of this voltage

from 3 to 12 V the output voltage of all the investigated converters increase nearly linearly. Note, that the dependences $\eta(V_{in})$, $T_T(V_{in})$ and $T_D(V_{in})$ are the increasing functions too.

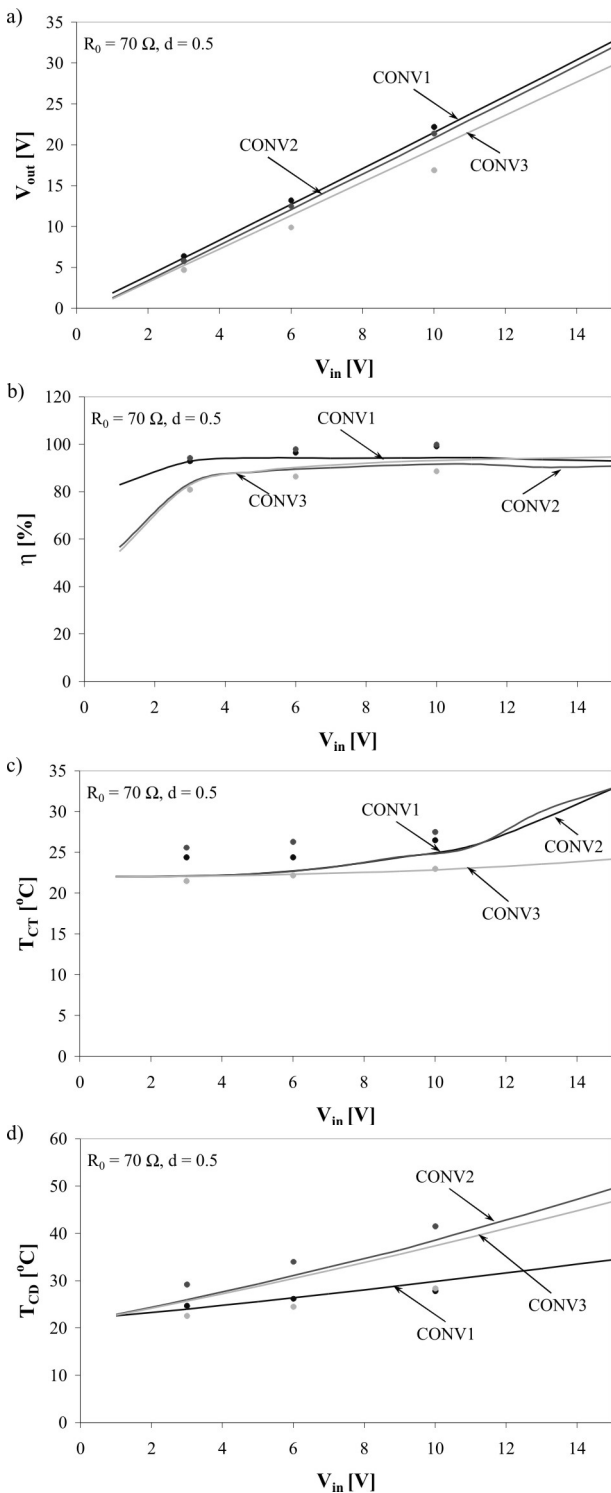


Figure 8: Dependences of the converter output voltage (a), the watt-hour efficiency (b), the transistor case temperature (c) and the diode case temperature (d) on the input voltage

In Figs.6-8 one can observe that the highest values of the converter output voltage and the watt-hour efficiency are observed for the converter CONV1 including silicon devices analysis. On the contrary, the highest values of transistor case temperature are observed for the converter CONV3, whereas the highest value of the diode case temperature was obtained for the converter CONV2. After using the SiC-MESFET, the considerable reduction of the output voltage and the watt-hour efficiency is observed. The described relationships were observed in a wide range of the pulse duty factor of the control signal and in a wide range of load resistance.

4. Conclusions

In the paper the results of the analyses and measurements of the characteristics of the boost converter with silicon and silicon carbide devices are presented. Due to the higher value of the resistance of the switched-on SiC transistor channel and a higher voltage drop on the SiC diode, the converter operating parameters have worse values when silicon devices are used. Therefore, the use of the SiC-devices in low-voltage dc-dc converters is unjustifiable.

The use of the hybrid electrothermal models of Schottky diodes and unipolar transistors allow obtaining a good agreement between the results of the analyses and measurements for all types of semiconductor devices (Si and SiC). This confirms the usefulness of these kinds of models in the analysis of the considered class of converters.

References

1. M. H. Rashid, Power Electronics Handbook, Elsevier, 2007.
2. R. Seyezhai, B.L. Mathur, Design and implementation of interleaved boost converter for fuel cell systems, International Journal of Hydrogen Energy, Vol. 37, No. 4, 2012, pp. 3897-3903.
3. D. Peftitsis, J. Rabkowski, G. Tolstoy, H.-P. Nee, Experimental comparison of dc-dc boost converters with SiC JFETs and SiC bipolar transistors, 14th European Conference on Power Electronics and Applications, EPE 2011; Birmingham, 2011.
4. A. Hensel, C. Wilhelm, D. Kranzer, Development of a boost converter for PV systems based on SiC BJTs, 14th European Conference on Power Electronics and Applications, EPE 2011, Birmingham, 2011.
5. M.M. Hernando, A. Fernández, J. García, D.G. Lamar, M. Rascón, Comparing Si and SiC diode

- performance in commercial AC-to-DC rectifiers with power-factor correction, *IEEE Transactions on Industrial Electronics*, 2006, 53 (2), pp. 705-707.
6. V.P. Galigekere, M.K. Kazimierzczuk, Effect of SiC Schottky and Si junction diode reverse recovery on boost converter, Electrical Insulation Conference and Electrical Manufacturing Expo, EEIC 2007; Nashville, 2007, pp. 294-298.
 7. B. Ray, R.L. Spyker, High temperature design and testing of a DC-DC power converter with Si and SiC devices, 39th Annual Meeting IEEE Industry Applications Society, Seattle, Vol. 2, 2004, pp. 1261-1266.
 8. K. Górecki, J. Zarębski, Modeling Nonisothermal Characteristics of Switch-Mode Voltage Regulators, *IEEE Transactions on Power Electronics*, 23 (4), 2008, pp. 1848 – 1858.
 9. C.N.M. Ho, H. Breuninger, S. Pettersson, G. Escobar, F. Canales, A comparative performance study of an interleaved boost converter using commercialized Si and SiC diodes for PV applications, 8th International Conference on Power Electronics - ECCE Asia: "Green World with Power Electronics", ICPE 2011-ECCE Asia 2011, 2011, pp. 1190-1197.
 10. J. Biela, M. Schweizer, S. Waffler, J.W. Kolar, SiC versus Si - Evaluation of potentials for performance improvement of inverter and DCDC converter systems by SiC power semiconductors, *IEEE Transactions on Industrial Electronics*, Vol. 58 (7), 2011, pp. 2872-2882.
 11. M.G.H. Aghdam, T. Thiringer, Comparison of SiC and Si power semiconductor devices to be used in 2.5 kW dc/dc converter, 2009 International Conference on Power Electronics and Drive Systems, PEDS 2009, Taipei, 2009, pp. 1035-1040.
 12. J. Biela, D. Aggeler, S. Inoue, H. Akagi, J.W. Kolar, Bi-directional isolated DC-DC converter for next-generation power distribution - Comparison of converters using Si and SiC devices, *IEEE Transactions on Industry Applications*, 128 (7), 2008, pp. 901-909.
 13. J. Zarębski, K. Górecki, K. Posobkiewicz, Influence of the use of silicon carbide semiconductor devices on characteristics of buck converters, *Przegląd Elektrotechniczny*, 86 (11a), 2010, pp. 229-231.
 14. J. Rąbkowski, R. Barlik, Three-phase inverter with SiC JFETs and Schottky diodes. *Przegląd Elektrotechniczny*, 86 (11a), 2010, pp. 116-119.
 15. A. Kadavelugu, V. Baliga, S. Bhattacharya, M. Das, A. Agarwal, Zero voltage switching performance of 1200V SiC MOSFET, 1200V silicon IGBT and 900V CoolMOS MOSFET, 3rd IEEE Energy Conversion Congress and Exposition ECCE 2011, Phoenix, 2011, pp. 1819-1826.
 16. A.M. Abou-Alfotouh, A.V. Radun, H.-R. Chang, C. Winterhalter, A 1-MHz hard-switched silicon carbide dc-dc converter, *IEEE Transactions on Power Electronics*, 2006, 21 (4), pp. 880-889.
 17. D. Aggeler, J. Biela, J.W. Kolar, A compact, high voltage 25 kW, 50 kHz DC-DC converter based on SiC JFETs, IEEE Applied Power Electronics Conference and Exposition - APEC 2008, Austin, pp. 801-807.
 18. M. Bhatnagar, B. J. Baliga, Comparison of 6H-SiC, 3C-SiC, and Si for power devices, *IEEE Transactions on Electron Devices*, 1993, 40 (3), pp. 645-655.
 19. R. Singh, J.A. Cooper, M.R. Melloch, T.P. Chow, J.W. Palmour, SiC power Schottky and PiN diodes, *IEEE Transactions on Electron Devices*, 2002, 49 (4), pp. 665-672.
 20. K. Lawson, S.B. Bayne, Transient performance of SiC MOSFETs as a function of temperature, *IEEE Transactions on Dielectrics and Electrical Insulation*, 18 (4), 2011, pp. 1124-1129.
 21. K. Sheng, Maximum junction temperatures of SiC power devices, *IEEE Transactions on Electron Devices*, 2009, 56 (2), pp. 337-342.
 22. P. Friedrichs, Silicon carbide power devices - status and upcoming challenges, *2007 European Conference Power Electronics and Applications*, 2007, pp. 1-11.
 23. T. Funaki, J.C. Balda, J. Junghans, A.S. Kashyap, F.D. Barlow, H.A. Mantooth, T. Kimoto, T. Hikiyara, Power conversion with SiC devices at extremely high ambient temperatures, IEEE Annual Power Electronics Specialists Conference PESC, 2005, pp. 2030-2035.
 24. J. Zarębski, J. Dąbrowski, Investigations of SiC merged pin Schottky diodes under isothermal and non-isothermal conditions, *International Journal of Numerical Modelling: Electronic Networks, Devices and Fields*, 24 (3), 2011, pp. 207-217.
 25. A. Elasser, T.P. Chow, Silicon carbide benefits and advantages for power electronics circuits and systems, *Proceedings of the IEEE*, 2002, 90 (6), pp. 969-986.
 26. M. Sekikawa, T. Funaki, T. Hikiyara, A study on power device loss of DC-DC buck converter with SiC Schottky barrier diode, 2010 International Power Electronics Conference - ECCE Asia, IPEC 2010, Sapporo, 2010, pp. 1941-1945.
 27. N. Mohan, W.P. Robbins, T.M. Undeland, R. Nilssen, O. Mo, Simulation of Power Electronic and Motion Control Systems – An Overview, *Proceedings of the IEEE*, 82 (8), 1994, pp. 1287-1302.
 28. D. Maksimovic, A.M. Stankovic, V.J. Thottuvelil, G.C. Verghese, Modeling and simulation of power electronic converters, *Proceedings of the IEEE*, 89 (6), 2001, pp. 898-912.

29. Ch. Basso, *Switch-Mode Power Supply SPICE Cookbook*, McGraw-Hill, New York 2001.

30. K. Górecki, J. Zarębski, Electrothermal analysis of the self-excited push-pull dc-dc converter, *Microelectronics Reliability*, 2009, 49 (4), pp. 424-430.

31. K. Górecki, Electrothermal compact model of CoolSET voltage regulators for SPICE, *International Journal of Numerical Modelling: Electronic Networks, Devices and Fields*, 20 (4), 2007, pp. 181 – 195.

32. M. K. Kazimierczuk, *Pulse-width Modulated DC-DC Power Converters*, John Wiley & Sons, 2008.

33. L.T. Su, D.A. Antoniadis, N.D. Arora, B.S. Doyle, D.B. Krakauer, SPICE model and parameters for fully-depleted SOI MOSFET's including self-heating, *IEEE Electron Device Letters*, 1994, 15 (10), pp. 374-376.

34. K. Górecki, Non-linear average electrothermal models of buck and boost converters for SPICE, *Microelectronics Reliability*, 49 (4), 2009, pp. 431-437.

35. K. Górecki, A New Electrothermal Average Model of the Diode-Transistor Switch, *Microelectronics Reliability*, 48 (1), 2008, pp. 51-58.

36. J. Zarębski, K. Górecki, J. Dąbrowski, Modeling SiC MPS diodes. *Proceedings of the International Conference on Microelectronics, ICM, Sharjah, 2008*, art. no. 5393829 , pp. 192-195.

37. J. Zarębski, D. Bisewski, DC characteristics of the SiC MESFETs, *Proceedings of International Conference Modern Problems of Radio Engineering, Telecommunications and Computer Science, TCSET 2006, Slavske, 2006*, art. no. 4404453 , pp. 87-89.

38. J. Zarębski, K. Górecki, SPICE-aided modelling of dc characteristics of power bipolar transistors with selfheating taken into account, *International Journal of Numerical Modelling Electronic Networks, Devices and Fields*, 22 (6), 2009, pp. 422-433.

39. P.A. Mawby, P.M. Igic, M.S. Towers, Physically based compact device models for circuit modelling applications, *Microelectronics Journal*, 2001, 32 (5-6), pp. 433-447.

40. M.A. Imam, M.A. Osman, A.A. Osman, Simulation of partially and near fully depleted SOI MOSFET devices and circuits using SPICE compatible physical subcircuit model, *Microelectronics Reliability*, 44 (1), 2004, pp. 53-63.

41. J. Zarębski, K. Górecki, The electrothermal large-signal model of power MOS transistors for SPICE, *IEEE Transaction on Power Electronics*, 25 (5-6), 2010, pp. 1265 – 1274.

42. F.N. Masana, SiC Schottky diode electrothermal macromodel, *17th International Conference - Mixed Design of Integrated Circuits and Systems, MIXDES 2010, Wrocław, 2010*, pp. 371-374.

43. E. Schurack, T. Latzel, A. Gottwald, SPICE-simulation of Nonlinear Effects in Filed-Effect-Transistors Caused by Thermal Power Feedback, *IEEE International Symposium on Circuits and Systems ISCAS 1993, Chicago, Vol. 2*, pp. 1116-1119.

44. J. Zarębski, K. Górecki, Influence of semiconductor devices on characteristics of the boost converter, *IX International Conference on Microtechnology and Thermal Problems in Electronics Microtherm 2011, Łódź, 2011*, pp. 279-284.

45. B.M. Wilamowski, R.C. Jaeger, *Computerized circuit Analysis Using SPICE Programs*, McGraw-Hill, New York 1997.

46. J. Zarębski, K. Górecki: A SPICE Electrothermal Model of the Selected Class of Monolithic Switching Regulators. *IEEE Transactions on Power Electronics*, Vol. 23, No. 2, 2008, pp. 1023 – 1026.

47. K. Górecki, J. Zarębski: Influence of MOSFET Model Form on Characteristics of the Boost Converter. *Informacije MIDEM*, 41, (1) 2011, pp. 1-7.

Appendix

The parameter values of the hybrid electrothermal models of the considered diodes and transistors are collected in Tables 1-4.

Table 1: Parameters values of the hybrid electrothermal model of the Si-MOSFET (IRF540)

Parameter name	Level	Gamma	Delta	Eta	Theta	Kappa	Vmax	Xj	Tox	Uo	Phi
Parameter value	3	0	0	0	0	0	0	0	100nm	600 cm ² /V/s	0.6 V
Parameter name	Rs	Kp	W	L	Vto	Rd	Rds	Cbd	Pb	Mj	Fc
Parameter value	16 mΩ	20.71 μA/V ²	0.94 m	2 μm	3.136 V	22 mΩ	444.4 kΩ	2.408 nF	0.8 V	0.5	0.5
Parameter name	Cgso	Cgdo	Rg	Is	N	Tt	R _{ON}	a _{RD}	R _{th}		
Parameter value	1.153 nF/m	445.7 pF/m	5.557 Ω	2.859 pA	1	142 ns	38 mΩ	0.012 K ⁻¹	12 K/W		

Table 2: Parameters values of the hybrid electrothermal model of the Si-Schottky diode (1N5822)

Parameter name	Is	Rs	Ikf	N	Xti	Eg	Cjo	M
Parameter value	100 nA	34.63 mΩ	2.37 A	1	0	1.11 V	1.032 nF	0.6736
Parameter name	Vj	Fc	Isr	Nr	a _u	a _{rs}	R _{th}	
Parameter value	0.75 V	0.5	9.599 mA	2	-2 mV/K	0.003 K ⁻¹	60 K/W	

Table 3: Parameters values of the hybrid electrothermal model of the SiC-Schottky diode (SDP04S60)

Parameter name	IS	RS	IKF	N	XTI	EG	BV	IBV	ISR
Parameter value	0.27 fA	190 mΩ	0	1.099	2.2	1.319 V	670 V	0.2 A	1.9 pA
Parameter name	NBV	NR	VJ	M	TRS1	TRS2	α _{rs}	α _u	R _{th}
Parameter value	1500	2.36	0.75 V	1	0.004 K ⁻¹	30x10 ⁻⁶ K ⁻²	0.005 K ⁻¹	-1.5 mV/K	30 K/W

Table 4: Parameters values of the hybrid electrothermal models of the SiC-MESFET (CRF24010)

Parameter name	Level	B	ALPHA	VTO	LAMBDA	BETA	VTOTC	RD	RS	RG	IS
Parameter value	2	26.6 V ⁻¹	0.135 V ⁻¹	-13.84 V	0.0085 V ⁻¹	0.5 A/V ²	-0.002 V/K	0.17 Ω	0.1 Ω	10 Ω	70 fA
Parameter name	N	CGS	CGD	CDS	VBI	VMAX	VDELTA	R _{ON}	α _{RD}	R _{th}	
Parameter value	1.25	6.7 pF	0.3 pF	1.3 pF	1.8 V	0.1 V	3 V	0.37 Ω	0.006 K ⁻¹	10 K/W	

Arrived: 16. 08. 2012

Accepted: 15. 10. 2012